Simulation of liquid impacts with a two-phase parallel SPH model

P.-M. Guilcher [(1)], G. Oger [(1)], L. Brosset [(2)], E. Jacquin [(1)], N. Grenier [(3)], D. Le Touzé [(3)]
[(1)]HydrOcean
Nantes, France
[(2)]Liquid motion dept, GTT (Gaztransport & Technigaz)
Saint-Rémy-lès-Chevreuse, France
[(3)]Ecole Centrale Nantes
Nantes, France

ABSTRACT

An SPH model of monofluid/structure interactions has already been integrated in a parallel solver named SPH-flow, and applied in the context of sloshing impacts (Oger et al., 2009). The developments carried out by *HydrOcean* and *Ecole Centrale Nantes* were supported by *GTT* (*Gaztransport & Technigaz)* for sloshing applications.

The formulation of SPH-flow has been recently extended as a result of this partnership, enabling the treatment of interactions between several fluids.

This paper presents the theoretical model of SPH-flow for the two-phase formulation. Applications to liquid impacts are given, confirming the strong influence of the gas on the flow evolution and impact pressure peaks.

The two first simulations proposed in the paper are a contribution to the numerical comparative study organized within ISOPE 2010: the mono-dimensional problem of a piston compressing a gas, and the free gravity fall of a bi-dimensional liquid patch through a gas. Finally, the simulation of a breaking wave impacting a rigid wall with a gas pocket entrapped is presented.

KEY WORDS: Sloshing, SPH, Liquid Impact, Compressibility, LNG carriers, Speed of sound, Fluid-Structure Interaction (FSI), Breaking Waves, CFD.

INTRODUCTION

The influence of the gas phase during a liquid impact event on a wall, such as a sloshing impact, appears to be crucial for a good estimation of the impact pressures. This has been confirmed experimentally by sloshing model tests when comparing statistical pressures obtained with gases of different densities within the tank (Maillard et al., 2009). When assumed as non condensable, the gas properties that matter during the liquid/gas interaction are mainly the density, and the compressibility (hence the speed of sound, whatever the equation of state that is considered).

As the membrane containment systems designer for LNG carriers, *GTT* (*Gaztransport & Technigaz)* continues to work on sloshing related R&D, to obtain improved predictions of their design loads. Numerical simulation is considered as a complement to experiments in order to get more insights on the physics of sloshing impacts. Such work enables parametric studies of impacts in ideal situations (simplified initial shape of the input wave, ideal physical properties of liquids and gases, simplified list of physical phenomena involved), that would not be possible by experimental analysis alone. Thus providing a further understanding of the physics of such problems.

Special attention has been paid to the Smoothed Particle Hydrodynamics (SPH) method. Indeed, the SPH method offers advantages over classical numerical methods when simulating sloshing type problems. No connectivity is required for the free surface, enabling the simulation of violent flows with possible fragmentation and interface reconnection. The Lagrangian formulation cancels the interface diffusion, resulting in a sharp definition of interfaces between gas, liquid and structure. Moreover, SPH method can be applied to any continuum description, resulting in an ability to easily approach multi-physics. Therefore, SPH method can theoretically solve in a fully coupled way, the compressible multi-phase structural interaction problem occurring during sloshing phenomenon.

After presenting the theoretical aspects of the SPH bi-fluid developments, applications to liquid impacts are presented.

SPH THEORY FOR BI-FLUID FLOWS

The developments to upgrade the SPH-flow software from a mono-fluid/structure parallel version to a bi-fluid/structure parallel version are described in this section.

Main characteristics of SPH-flow software

SPH-flow is a 2D and 3D parallel SPH solver developed by *Ecole Centrale Nantes* and *HydrOcean* (Doring, 2005) (Oger, 2006) (Deuff, 2007) (Guilcher, 2008) (Grenier, 2009). It enables solving complex fluid and multi-physics problems through massive HPC resources. Complex geometries in free or forced motions can be modelized with a variable space discretization (variable-H) solver for increased resolution simulations.

The solver was first developed for fluid flow simulations dedicated to complex non-linear free surface problems. Within this context, the

conservation laws for a compressible fluid are solved, together with the Tait equation of state. Inspired by Finite Volume formalisms, Vila (Vila, 1999) proposed to rewrite the SPH formalism initially developed by Monaghan (Monaghan, 1992). A Riemann solver in a Lagrangian framework was introduced, leading to increased stability properties of the scheme. Combined with the MUSCL (Monotone Upwind Centered Scheme for Conservation Law) extrapolation (Van Leer, 1979), this scheme provides very stable and low-diffusive results and can be written in the more general Arbitrary-Lagrange-Euler (ALE) formalism. Accuracy and convergence order of the scheme have been increased, leading to upgraded spatial derivatives determination by using a weight renormalization matrix (Vila, 1999).

Through the use of a linear equation of state for pressure and the adjunction of a deviatoric part in the stress tensor, the solver was easily adapted to structure simulations (Deuff, 2007) and made it possible to reach interesting results (Oger et al., 2009) with GTT's containment systems. Up to now, only the linear elasticity model has been implemented and validated.

Despite the use of new improvements such as Riemann solvers or renormalization techniques, a numerical instability, specific to meshless methods, cannot be completely eliminated (Swegle et al., 1995). This so-called 'tensile instability' grows when the continuum is under tension. It may lead to unrealistic numerical fractures in areas of intense stress rates, even under the elastic deformation assumption. Therefore, specific algorithms such as Lagrangian kernels (Rabczuk et al., 2004) (Bonet et al., 2001) and artificial stress tensors (Gray et al., 2001) have been introduced in the SPH-flow solver, in order to cope with this complex instability (Oger et al., 2009).

The last step was to couple the above SPH models for fluids and structures in order to enable Fluid/Structure Interactions (FSI). This work was first achieved through a PhD Thesis (*GTT / ECN*) (Deuff, 2007). The work was implemented in the SPH-flow platform. The kinematic and dynamic conditions at the fluid/structure interface are fulfilled.

A parallel version of SPH-flow including the fluid and structure solvers as well as the FSI model has been developed. It is based on a domain decomposition strategy, and uses MPI as the inter-node communication standard. As shown in Figure 1, linear and even super-linear speedups are obtained, due to large cache effects (cache miss reduction). More generally, an efficiency rate from 70% to 90% (depending on the problem to solve and the number of particles and processes involved) is commonly reached.

Today, the calculations usually performed by *HydrOcean* involve 16 processors so that a calculation that lasted 1 week in sequential computation is now performed in half a day.

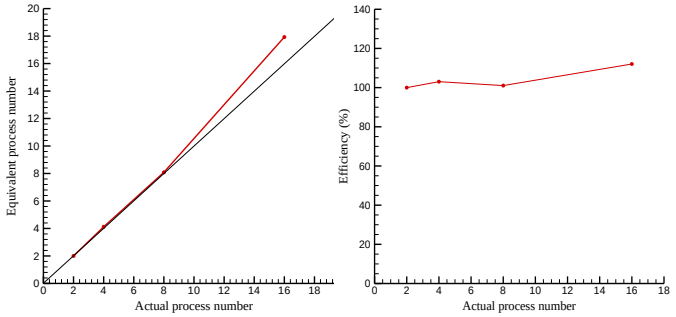

***Fig. 1** - Parallelization speed-up and efficiency for a FSI problem involving 430,000 particles with from 2 to 16 processes.*

The different possible models for bi-fluid flows

An overview of the current developments in the area of meshless methods dealing with two-phase formulations is now presented.

Lagrangian meshless methods display a significant advantage over classical mesh-based methods: the Lagrangian motion of particles enables non-diffusive, thus very sharp, interfaces. However, like most numerical methods, SPH encounters difficulties when dealing with very different fluid densities, like in the case of gas-liquid problems.

For a few years, several SPH models have been proposed to simulate interfacial flows. The first one (Colagrossi et al., 2003) was based on a classical SPH scheme with artificial upwind viscosity. Numerical results are in good agreement with available data for a large range of gas to liquid density ratios, going from 0.001 to 0.5 and for impact problems. Nevertheless, practical stability considerations impose to take large unphysical speed of sound for the light phase. Thus, the numerical scheme is not well adapted to large compression of the gas.

A second model, proposed by (Hu et al, 2006), deals with large discontinuities of density at the interface through a specific treatment avoiding density kernel smoothing. This scheme shows good results for academic test cases with slow dynamics in incompressible flows.

The last approach, adapted from Eulerian Finite Volume Schemes, relies on the use of a volume fraction for each particle (Cueille, 2005), (Grenier, 2009). All the phases coexist within a particle and the mixture of phases is controlled via the volume fraction. For instance, the volume fraction represents the percentage of water of the particle, the residual being the percentage of air. As a consequence, a particle cannot be only pure water or pure air. Unlike the other SPH two-phase schemes, this volume fraction SPH scheme cannot avoid numerical diffusion at the interface. However, the diffusion can be significantly reduced by using the Lagrangian framework. Simplified linearized Equations of State are used to reduce the scheme complexity.

Among all these existing schemes, it appears difficult to handle in the same formalism the different features involved in a sloshing impact: fast dynamics, significant compressibility effects, large difference between the fluid densities, use of real physical properties. The numerical scheme selected for liquid impact problems in presence of gas fulfils all these requirements. It is presented in the next sub-section.

A bi-fluid SPH model well adapted for liquid impact problems

The SPH model selected is based on an interface treatment first proposed by Leduc (Leduc et al., 2009), enabling very small density ratios and realistic values for the speeds of sound.

The system of conservation laws for isentropic Euler equations is considered in conservative form in each phase:

$$L_{\vec{v}_o}(\Phi) + div\,(F_E(\Phi) - v_o\Phi) = S \tag{1}$$

Φ is the vector of conservative variables, F_E the Eulerian flux matrix and S the volumic source term. The system of equations is written here in an arbitrary moving reference frame (Arbitrary-Lagrange-Euler (ALE) description) where v_o denotes the transport velocity field.

$$\Phi = \begin{pmatrix} \rho \\ \rho v^{(1)} \\ \rho v^{(2)} \end{pmatrix}, \quad F_E{}^{(1)}(\Phi) = \begin{pmatrix} \rho v^{(1)} \\ \rho v^{(1)} v^{(1)} + p \\ \rho v^{(1)} v^{(2)} \end{pmatrix}, \quad F_E{}^{(2)}(\Phi) = \begin{pmatrix} \rho v^{(2)} \\ \rho v^{(1)} v^{(2)} \\ \rho v^{(2)} v^{(2)} + p \end{pmatrix} \tag{2}$$

To close the system, a generic Tait Equation of State relating pressure to density is used:

$$p = \frac{\rho_0 a_0^2}{\gamma}\left(\left(\frac{\rho}{\rho_0}\right)^{\gamma} - 1\right) \tag{3}$$

ρ_0, a_0 and γ are respectively the nominal density, the nominal speed of sound and the isentropic constant for the considered fluid.

The fluid domain is discretized by a set P of particles. Each particle i has a location x_i, a volume of control w_i and carries its own properties

(velocity, pressure, etc.). A weak form of discretization associated to (1) by use of SPH spatial derivative operators leads to the following scheme for Euler equations:

$$\frac{d}{dt}(w_i\Phi_i) + w_i \sum_{j\in P} w_j 2G(\Phi_i, \Phi_j, n_{ij}) B_{ij} \cdot \nabla W_{ij} = w_i S_i \quad (4)$$

The volume deformation along trajectories becomes:

$$\frac{dw_i}{dt} = w_i \sum_{j\in P} w_j (v_j^o - v_i^o) \cdot B_{ij} \cdot \nabla W_{ij} \quad (5)$$

The transport equation becomes : $$\frac{dx_i}{dt} = v_i^o \quad (6)$$

The upwind numerical flux *G* is given either by exact or approximate Riemann solvers in the moving framework. Extension to second order with MUSCL algorithm is performed with linear reconstruction on pressure and velocity. The term B_{ij} stands for the symetrized renormalization matrix (Vila, 2005).

The Ordinary Differential Equations (4) to (6) are marched in time with classical 4th order Runge-Kutta scheme, or 3rd order Strong Stability Preserving Runge-Kutta scheme. Time step is restricted by a CFL-like condition on acoustic waves.

A specific treatment is applied at the interface between two fluids. The mono-fluid Riemann solver is replaced by a multi-fluid linearized approximate Riemann solver. The Riemann problem relies on the continuous variables across interface, namely the pressure and the normal velocity, instead of using the conservative variables. Moreover, the upwind velocity resulting from the Riemann solver is used together with the ALE framework in order to block mass transfers between the fluids. Thus, Lagrangian form of the ALE formalism is implicitly assumed at the interface. The equation for volume evolution becomes:

$$\frac{dw_i}{dt} = w_i \sum_{j\in P} w_j (v_E^*(x_{ij}) - v_i^o) \cdot B_{ij} \cdot \nabla W_{ij} \quad (7)$$

Where $v_E^*(x_{ij})$ is the upwind velocity at contact discontinuity resulting from the Riemann problem between particles *i* and *j*.

Implementation of the bi-fluid model in SPH-flow

The implementation within the SPH-flow platform of the bi-fluid formulation, described in the previous sub-section, required a complete compatibility with the functionalities developed formerly. Fluid-structure interaction problems must be solved, possibly involving several materials and several fluids in a global homogeneous framework. The parallelization efficiency is to be conserved.

In order to cope with these constraints, a global generic formulation for any fluid had first to be developed. Apart from the Godunov solver, expressions (4) to (6) remain the same whatever the fluid studied. So, the first development concerned a generic Godunov solver for any fluid. The solver automatically adapts to the fluid properties (ρ_0, γ and c_0). The SPH method is particularly well-developed to such adaptations since the fluid properties are carried by each particle all along the calculation.

On the other hand, the Godunov solver for structures could not be the same as for fluids. Hence, two solvers must to coexist: one corresponding to the linearized Equation of State for structure, and the other for the Tait Equation of State for fluids. Now, when some particles owned by two different fluids interact together, the bi-fluid interface model is applied. Finally, when a fluid particle interacts with any material particle, conditions at the interface described in (Oger et al., 2009) are automatically fulfilled, enabling fluid-structure coupling in problems involving several fluids and structures together.

Thus, the overall parallel framework of SPH-flow remains unchanged, keeping the same speedup and efficiency properties for this resulting multi-phases/multi-species parallel SPH solver.

APPLICATIONS TO LIQUID IMPACTS

The developments described in the previous sections have been made very recently. In this section, the first application of the bi-fluid version of SPH-flow concerning liquid impacts is presented. Several improvements still need to be made. For example, some void cavities tend to appear spontaneously in fluid regions with low pressures, as in the vortex areas. This phenomenon seems to be very comparable in nature to the classical Tensile Instability.

The 1D and 2D calculation cases based on the geometries proposed for the Numerical Comparative Study organized within ISOPE 2010 (see Dias et al., 2010) are first presented. As the 1D case is a simple problem that can be solved semi-analytically, the comparison with the reference solution can be considered as a validation as far as simple compressions of entrapped gases (without any escape) are concerned. A more realistic simulation of a 2D breaking wave impacting a wall, while entrapping a gas pocket is presented. The same simulation had been presented last year with the mono-fluid version (Oger et al., 2009).

The 2D results presented are to be considered as preliminary. For time saving consideration, the adopted density of particles is too small to hope for a realistic determination of the impact pressures. Nevertheless some realistic trends are observed.

1D compression of a gas column

The 1D calculation cases correspond to the gravity drop of a liquid segment along a vertical line (1D tank). At the initial instant, the liquid is at rest and is surrounded by gas above and underneath it, at atmospheric pressure, as shown in Figure 2. No flow outside the line direction is allowed. This corresponds to an idealization of the free fall of a liquid piston within a vertical cylinder, very close to the Bagnold problem (Bagnold, 1939).

This problem is simple enough to enable a semi-analytical approach assuming a perfect gas and an isentropic process, which are also the assumption in the software for the time being. The theoretical formulation leads to a first order differential equation integrated numerically. The solution used here was proposed by F. Dias of *Ecole Normale Supérieure Cachan (Fr)* (Dias, 2008).

It is shown in Braeunig et al (2010), that the problem can be defined in a dimensionless form thanks to a dimensionless parameter S:
$S = \rho_l\ g\ h/p_0$, where ρ_l is the liquid density, which measures the violence of the impact through the parameters of the inflow conditions (global flow) is named *Impact number*.

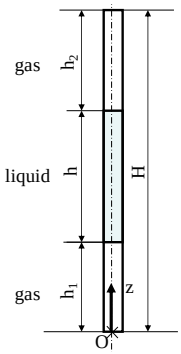

Length	(m)
H	15
h	8
h_1	2
h_2	5

***Fig. 2** – 1D reference case for the numerical benchmark of ISOPE2010. Main geometrical characteristics at scale 1.*

Several calculations have been made, based on this simple geometry, varying either the properties of the fluids or the geometrical scale. The

calculation matrix is shown in Table 1.

Table 1 *– Calculation matrix for the 1D geometry in Fig. 2*

Case	Scale	Gas Dens.	Liq. Dens.	Dens. Ratio	Gas SoS	Liq. SoS	Gamma	Impact Number
Scale 1								
R1	1	1	1000	.0010	300.00	1500.00	1.16	1.01
R2	1	4	1000	.0040	300.00	1500.00	1.16	0.25
R3	1	50	1000	.0500	300.00	1500.00	1.16	0.02
R4	1	2	500	.0040	300.00	1500.00	1.16	0.25
Scale 1/40 with Partial Froude Scaling (PFS)								
PFS1	1/40	1	1000	.0010	300.00	1500.00	1.16	0.0253
PFS2	1/40	4	1000	.0040	300.00	1500.00	1.16	0.0063
PFS3	1/40	50	1000	.0500	300.00	1500.00	1.16	0.0005
PFS4	1/40	2	500	.0040	300.00	1500.00	1.16	0.0063
Scale 1/40 with Complete Froude Scaling (CFS)								
CFS1	1/40	1	1000	.0010	47.43	237.17	1.16	1.01
CFS2	1/40	4	1000	.0040	47.43	237.17	1.16	0.25
CFS3	1/40	50	1000	.0500	47.43	237.17	1.16	0.02
CFS4	1/40	2	500	.0040	47.43	237.17	1.16	0.25

SoS : Speed of Sound

Three series of four calculations were carried out. The first series corresponds to the calculations at scale 1 with four different densities of gas. The very high gas density ρ_g=50 kg/m^3 used in R_3 corresponds to an unrealistic gas. The case R_4 corresponds to the same density ratio as for R_2 but with different liquid and gas. When varying the density of gas, and keeping constant the speed of sound and the isentropic constant, the code will actually update the ullage pressure p_0 through the equation of state. The range of the parameters studied at scale 1 corresponds to a range from 0.25 to 1.01 of the Impact number. Case R_4 has the same Impact number as case R_2 and theoretically leads to the same results.

The second series repeats the same conditions as the first series with the same fluids, but at scale 1:40 (scale used in GTT for sloshing model tests). These conditions are referred to as *Partial Froude Scaling* (PFS) conditions because the impact conditions are Froude-scaled, except the properties of the fluids (Braeunig et al., 2009). The Impact numbers are λ=40 times smaller than the corresponding Impact numbers at scale 1 (S_λ=S/λ). The third series repeats the same conditions at scale 1:40 but with scaled properties of the gas and liquid. It is referred to as *Complete Froude Scaling* (CFS): the Impact number is kept the same as the respective Impact number at scale 1, and the results are expected to be also the same according to the theory.

A convergence study was made for the case R_1, increasing progressively the number of particles with a constant repartition along the complete length of the model. Results are presented in Figure 3 in terms of the pressure history at the bottom level, for four different models corresponding to a decreasing inter-particle distance (Δx) from 0.5, 0.25, 0.125 to 0.0625m (with respectively 30, 60, 120, 240 particles).

The four curves are very close and only a zoom-in around the crest enables to differentiate them clearly. So, for this simple case, the solution seems robust. The model with 120 particles was adopted for all calculations.

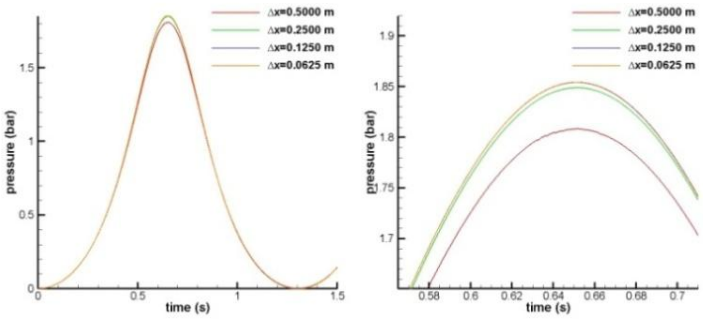

Fig. 3 *– Convergence study. Left: pressure time traces at the bottom for 4 different densities of particles. Right: zoom at the crest level.*

All results corresponding to the cases in the calculation matrix of the Table 1 are summarized in Figure 4. Four sub-figures are displayed referring to the four combinations of liquid and gas densities for each series in Table 1. For each sub-figure, three curves are displayed corresponding to the three series (scale 1, PFS, CFS). The results at scale 1/λ (λ=40) are Froude-scaled (time multiplied by $\sqrt{\lambda}$; pressure multiplied by $\lambda.\rho_l/1000$, ρ_l being the liquid density for the studied case)

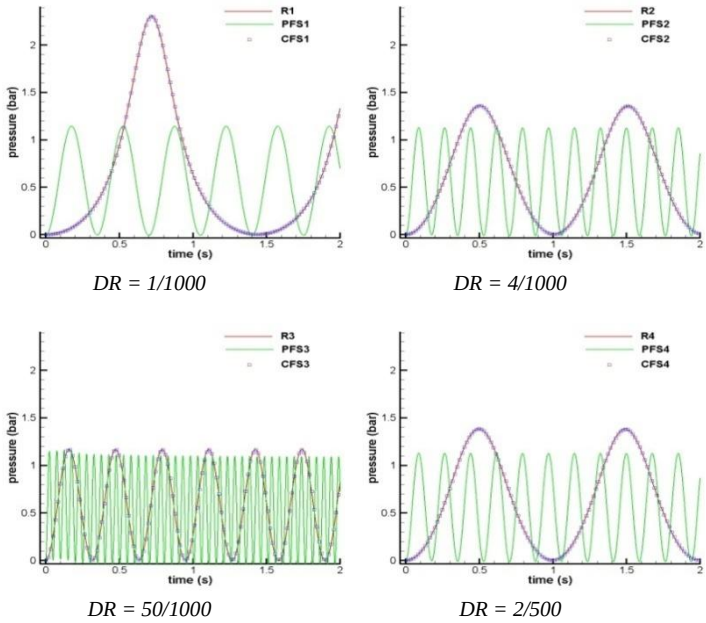

DR = 1/1000 *DR = 4/1000*

DR = 50/1000 *DR = 2/500*

Fig. 4 *– Pressure at the bottom of the 1D model for different density ratios. - Scale 1 (red), PFS (green), CFS (blue).*

The CFS results (dots in blue) at scale 1:40 match perfectly the results at scale 1 (curves in red) as explained in Braeunig et al. (2009). On the other hand, the PFS conditions (curves in green) can give results, after Froude-scaling, far from the corresponding results at full scale. The oscillations at small scale with the PFS conditions are quicker than at full scale, and the maximum pressures are reduced. At small scale the pressure time traces correspond to sine curves for whatever the Impact number S. At scale 1, the peak pressures are more important when the Impact number is larger.

Two different regimes of impacts seem to exist with a transition between them. There are the hard impacts with sharp pressure peaks and the soft impacts with sine behavior of the pressure histories. When decreasing the scale with PFS conditions, the second regime (soft impacts) is favored. So-called compressibility bias at small scale when PFS is applied is confirmed. When increasing the density ratio at a given scale the second regime is also favored.

Moreover, the results obtained for different liquids and gases keeping the same density ratio (thus the same Impact number) match completely, whatever the scale or the scaling conditions, according to Figure 4 for DR=4/1000 and DR=2/500. This is in agreement with the theory and validates the use of the correction factor for the pressure scaling given by the scale in liquid density ($p^{fs} = (\rho_L{}^{fs}/\rho_L{}^{ms}) \,.\, \lambda \,.\, p^{ms}$, *fs* and *ms* referring to full and model scales respectively), whatever the ratio of density.

The numerical SPH results match perfectly with the semi-analytical model of F. Dias. Whatever the studied condition, the two pressure time traces superimpose perfectly. Figure 5 summarizes the comparison between the two methods: the maximum dimensionless pressure $(p-p_0)/p_0$ is given with regards to the Impact number at the two scales.

The dots obtained with SPH-flow superimpose almost perfectly with the theory whatever the scale.

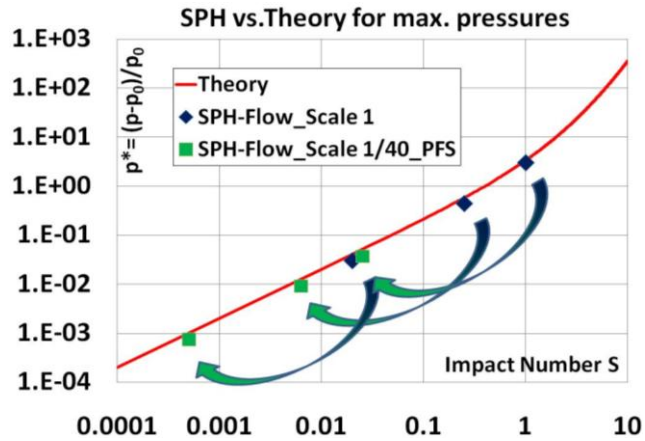

Fig. 5 *– Comparison between SPH-Flow results and semi-theoretical results for the 1D compression of a gas column – dimensionless pressure $(p-p_0)/p_0$ vs. Impact number S*

Going from full scale to model scale, with Froude-similar inflow conditions but without scaling the fluid properties (PFS), leads to multiply the Impact number by the scale ($S_\lambda=S/\lambda$). This is described schematically by the arrows on Figure 5. Doing so will strongly mitigate the impacts.

A detailed analysis of such a 1D compression of a gas pocket is proposed in Bogaert et al., (2010) and also in Braeunig et al. (2010), but taking into account the phase transition influence in the latter. The consequences on the Sloshing model tests are also analysed.

The SPH bi-fluid model can be considered as validated as far as simple compressions of entrapped gases (without any escape) are concerned.

2D free fall of a liquid rectangle in a rectangular tank filled with gas

A liquid patch initially rectangular at rest is surrounded by a gas in a rectangular tank. Initially at rest, it falls freely under gravity. The liquid impacts the rigid bottom of the tank. The main geometrical characteristics at full scale are depicted in Figure 6. This calculation case was studied first by Braeunig et al. (2009).

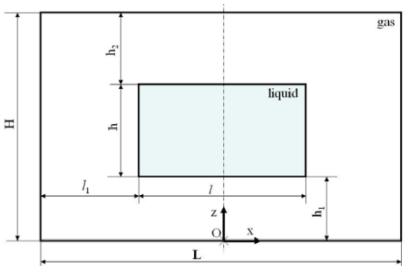

Length	(m)
H	15
h	8
h_1	2
h_2	5
L	20
l	10
l_1	5

Fig. 6 *– 2D reference case for the numerical benchmark of ISOPE 2010. Main geometrical characteristics at scale 1*

Four calculations were made, based on this simple geometry, varying either the properties of the fluids or the geometrical scale. The calculation matrix is shown in the Table 2. Although referring to the same geometry, the cases studied here do not match exactly with those of the ISOPE Numerical Study.

Case R_1 corresponds to water and air at scale 1. Case R_2 corresponds to gas and liquid matching the target density ratio of NG in equilibrium with LNG. Case PFS_1 corresponds to R_1 at scale 1/40, keeping the same liquid and gas properties as at scale 1 (*Partial Froude Scaling*). Case CFS_1 corresponds to R_1 in *Complete Froude Scaling*. Here, the scaling of the fluid properties is obtained by Froude-scaling the speeds of sound in both the liquid and the gas, keeping constant the adiabatic constant. In the perfect gas considered, as the speed of sound is Froude-scaled at constant density, the ullage pressure is automatically Froude-scaled by the relation (3).

Table 2 *– Calculation matrix for the 2D geometry in Fig. 6*

Case	Scale	Gas Dens.	Liq. Dens.	Dens. Ratio	Gas SoS	Liq. SoS	Adiabatic Cst
R1	1	1.2	1000	.0012	343.00	700.00	1.40
R2	1	4	1000	.0040	343.00	700.00	1.40
PFS1	1/40	1.2	1000	.0012	343.00	700.00	1.40
CFS1	1/40	1.2	1000	.0012	54.23	111.00	1.40

SoS : Speed of Sound

The speed of sound in the *real* gas was set at 343 m/s, which corresponds to the SoS of air at ambient conditions. The speed of sound in the *real* liquid was set at a low value (700 m/s) in order to accelerate the calculations (CFL condition). This should not influence much the results so long as the impacts studied are smooth.

A convergence study was performed for progressively increasing the densities of particles. The results are shown in Figure 7 for the case R_1. The pressure time traces at the centre of the bottom line are compared for three densities of particles, corresponding to a minimum distance between the particles at rest going from 10 cm to 2.5 cm. The Braeunig's results for the case R_1 were added to the Figure 7. The rectangular meshing, considered by Braeunig, was regular with square cells of 10 cm.

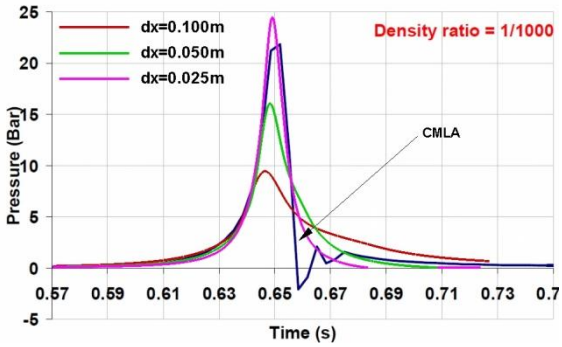

Fig. 7 *– Comparison for case R_1 between Braeunig's results(blue) and SPH-flow for increasing min particle distance dx - Pressures at the centre of the bottom line.*

The evolutions of the pressure pulses with SPH-flow for the different particle densities clearly show that convergence is not reached. The highest density studied, with the minimum distance of 2.5 cm between the particles is still too low. This is not really a surprise when trying to capture such sharp dynamic phenomenon.

This conclusion stands also for the Braeunig's results, for which the pressure pulse matches quite well the pressure pulse obtained with our highest density of particle. Actually, the undersizing pressure of the meshing was mentioned by the author.

Nevertheless this good matching in both the maximum pressure and the duration is rather a good sign.

This study is to be taken as mainly qualitatively indicative as some developments are still on-going to improve the bi-fluid SPH model. The tests will have to be run again after these developments for our best absolute evaluation of impact pressures. So, it was decided to use the smaller density of particles for all later calculations in order to shorten their duration. The maximum impact pressures that will be displayed later are thus under-estimated.

Taking benefit of the vertical symmetry of the problem, only half of the tank is really modelized. The model consists of 15,000 particles (for one half of the tank). The minimum distance between the particles at the initial time is 0.1 m. An average calculation case from the test matrix is performed in 1 hour for 0.75 s of real flow simulated on

16 processors (Dual Core Intel Xeon 5160 processors cluster).

Main characteristics of the flows are common for the different cases of the Table 2. They are illustrated in Figure 8 by four snapshots at four different instants displaying both the pressure and the velocity modulus for the case R_1 (water and air at full scale).

First, the liquid patch begins to fall under gravity, progressively moving the gas (Figure 8 – top-left). When the liquid comes close to the wall, the gas has to escape quicker and quicker remaining uncompressed (Figure 8 – top-right). The gas velocity is particularly important at the corners of the liquid patch (up to 110 m/s), leading to the apparition of vortices. Only in the last stage, the gas is compressed and the pressure calculated at the bottom centre rises. The wave pressure propagates through the liquid (Figure 8 – bottom-left). A thin layer of gas remains entrapped between the liquid and the bottom. This punctured pocket of gas pushes back the liquid (depending on the density ratio). The free surface bends under the gas pressure (Figure 8 – bottom-right).

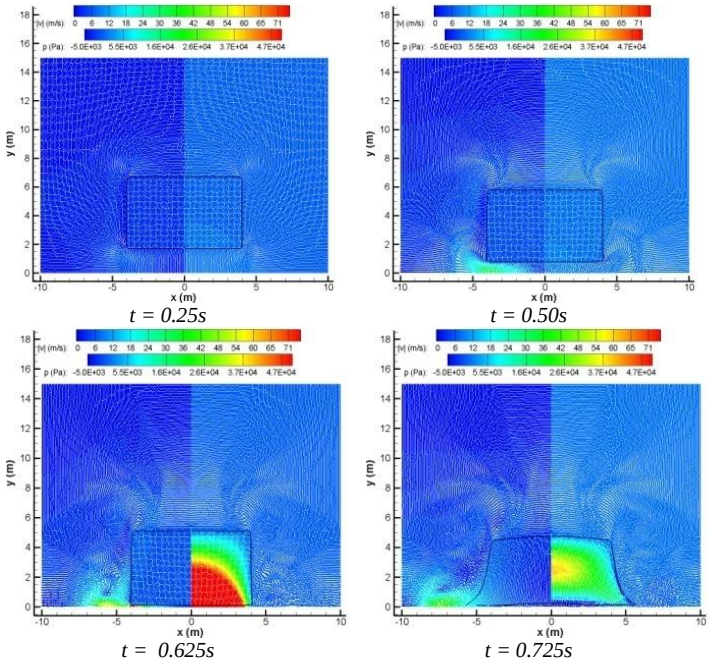

Fig. 8 *– Velocity and pressure for case R_1 (water and liquid at scale 1) at four different times. Each snapshot gives the velocity modulus (left) and the pressure (right). The line represents the interface between fluids.*

Influence of Density Ratio at scale 1 can be illustrated by the results from cases R_1 and R_2. They correspond to the increase gas densities (1.2 and 4) with the same liquid (water) at scale 1.

Figure 9 (left) presents the pressure time traces as calculated at the centre of the bottom wall in both cases. On the right side, it presents the time history of the interface velocity at the center vertical.

The maximum pressure is significantly smaller (around 30%), while the duration of the pulse is larger for the density ratio of 4/1000, compared with results for the density ratio of 1/1000. This is in good qualitative agreement with the general statistical observations made by GTT from the numerous sloshing model tests accumulated with either water and air, or with water and a mixture of gas of density 4 kg/m^3.

With real gases, the choice of different gases, in order to have different density ratios, would lead at the same time to different compressibility properties. It would not be possible to distinguish between the influence of the density ratio and the influence of the gas compressibility. Here, with virtual gases, the two effects can be clearly distinguished as only the density ratio differs.

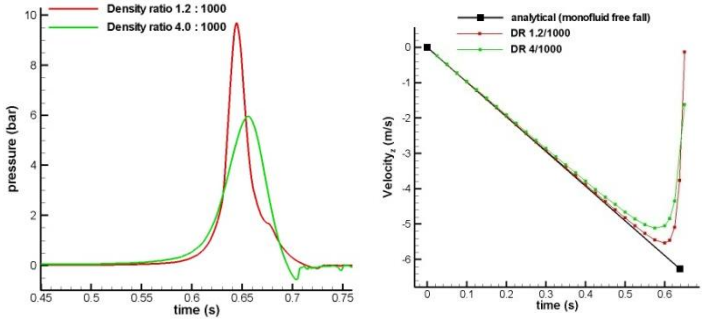

Pressure time history *Velocity of the interface at the centre line*

Fig. 9 *–Influence of Density Ratio (DR) at scale 1. DR=1.2/1000 (red) – DR=4/1000 (green).*

It is important to understand that the difference between the two cases does not appear immediately after the pressure rises (about 0.55 s from Figure 9). It starts with the escaping phase of the gas when the liquid falls and the gas can thus be considered as uncompressed. Between the bottom free surface of the liquid rectangle and the bottom wall, there is a gas pipe, for which the section is decreasing progressively while the liquid falls. When passing from a given height to a lower one, the free surface moves thus the same gas volume whatever the density ratio, so the moved mass is different. There is a transfer of momentum from the liquid to the gas, which will slow down the liquid fall and accelerate the gas escape. The heavier is the gas, the more rapid the deceleration of the liquid. This deceleration characteristic of the liquid is illustrated in Figure 9 (right).

It is interesting to notice that the liquid deceleration can be detected before the pressure rise, thus before any compression of the gas occurs. The difference between the two velocities is maximum, approximately at the instant when the two velocities reach maximum magnitude. The largest difference in magnitude is about 40 cm/s for a mean velocity around 5 m/s. This is to be considered as significant especially as the max pressure varies with the square of the velocity. The maximum horizontal velocity in the light gas is 110 m/s while it is 11 m/s in the heavy gas, corresponding to a ratio of 10.

At least qualitatively, the phase of gas escaping seems correctly simulated by SPH flow.

This kind of simulation helps to understand the notions of *Global Flow* and *Local Interactions during impacts* (see for example Braeunig et al., 2009 or Bogaert et al., 2010), which is important to understand how far the experimental model given by sloshing model tests is relevant.

The free fall is obviously governed mainly by the influence of gravity. Changing the liquid or the gas will not modify the overall fall of the liquid during its main duration until the interaction with the gas becomes significant. This interaction comes from, first the transfer of momentum between the liquid and the uncompressed gas (P_2 phenomenon according to Braeunig's classification), and then with the compression of the gas (P_5 according to Braeunig). The global flow could be defined as the phase until there is a starting deviation compared to the case with vacuum. It is more relevant to include P_2 into the definition of the global flow as its influence is rather global. With this definition, the global flow ends when the local interactions (first of all the compressibility of the gas) become influent. Such a definition is relevant with the change of scale. Indeed using software dealing only with uncompressible flows, it is easy and quick to show that the flows are Froude-similar at both scales only if both the Froude and the density ratio numbers are kept the same at both scales.

Scaling effects can be addressed by comparison between cases R_1, PFS_1 and CFS_1. The small scale of 1:40 adopted for PFS_1 and CFS_1 refers to the scale of the sloshing model tests in GTT.

Figure 10 shows the results for the three cases in terms of pressure time histories at the centre of the bottom wall. The results obtained at scale 1/40 are Froude scaled.

There is a perfect match between the red (full scale, R_1) and the green curve (Complete Froude scaling, CFS_1). On the contrary, adopting the Partial Froude scaled conditions at small scale (PFS_1) leads to significantly different results at both scales after Froude scaling. This means that the gas properties have to be scaled as stated in Braeunig's paper, to ensure that the gas compressibility acts in the same way regarding gravity effects for both small and full scales.

Oscillations can be observed clearly in Figure 10 with the PFS1 conditions at small scale. These oscillations are absent in the full scale pressure signal. This is the signature of a gas pocket oscillating as a mass/spring system. The different signatures at both scales show that the impacts are different. Keeping the same gas at both scales leads to exagerate the compressibility influence at small scale.

It is not useful to repeat the phenomenological analysis already done by Braeunig et al. in 2009. Obviously, this kind of results has some consequences on the sloshing model tests ability to provide a realistic representation. Here also the reader is advised to refer to the Braeunig's paper.

The simulations with SPH-flow seem to be able to capture qualitatively the compressibility bias induced at small scale by a partial Froude scaling.

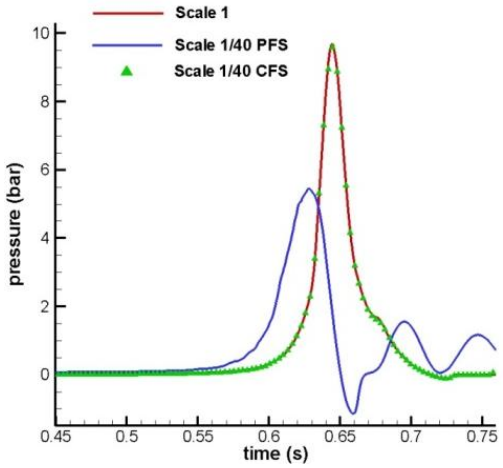

Fig. 10 *–Scaling effects – Pressure time traces at the centre of the bottom line. Scale 1 water & air (red), scale 1/40 PFS (blue), scale 1/40 CFS (green). Results at scale 1/40 are Froude-scaled.*

Wave breaking onto a rigid wall

The previous applications were academic. The application of a unilateral breaking wave impacting a rigid wall, presented in this sub-section, is more realistic. It is particularly relevant as such impacts are representative of sloshing impacts inside LNG tanks for low filling levels and these impacts are the cause of the highest impact pressures according to sloshing model tests. Moreover GTT has accumulated reliable experimental databases of such impacts obtained in different flume tanks at different scales (see Kimmoun et al., 2010), including full scale with the real containment systems fixed to the wall (see Brosset et al., 2009, Bogaert et al., 2010). The main objective of the developments presented in this paper, is to obtain a reliable numerical model of such breaking wave impact taking into account the influence of the gas (which is considered as crucial) and the influence of the containment system structure. The model must be accurate enough to capture very locally, the sharp peak pressures that are observed during the tests. With such a tool, it will be possible to study deterministically the scaling effects and the fluid-structure interaction influence (hydro-elasticity). Such an objective is also targeted directly with the tests but the technical difficulties to solve in order to enable the deterministic approach are possibly higher with the tests as described in Kimmoun's and Bogaert's papers. Both approaches followed at the same time will give us more chance to succeed.

Before performing large calculations with very refined densities of particles, which will lead to very long duration calculations, we are now in the process to check the ability of the code to capture the different phenomenon involved adequately. The fluid-structure interaction functionality is ready. The issue of the tensile instability is solved by the Lagrangian kernel (Oger et al., 2009). The wave breaking process has been simulated successfully in a mono-fluid context with refined density of particles enabling to capture very sharp impact pressures (Oger et al., 2009). For the compressible bi-fluid functionality, there are still issues to be solved that are very much related to the tensile instability although developing into the fluid and especially the light phase and requiring new solutions.

It would be completely inadequate to use the SPH code or any CFD software in order to simulate the propagation of a wave generated by a focusing process in a wave flume (the global flow). The propagation phase can be solved accurately by software based on potential theory (BEM for example), much faster than by CFD. However, such potential-theory-based software can obviously not simulate the local interactions between liquid, gas and structure that happen during impacts. Therefore, the strategy developed by GTT and HydrOcean is based on a coupling between two codes sharing the different tasks. A potential-theory based code is in charge of the global flow and SPH-flow is in charge of the local interactions simulations during the impact in the vicinity of the impacted wall. The SPH calculations are restricted in a rectangular domain adjoining the wall. As shown in Figure 11.

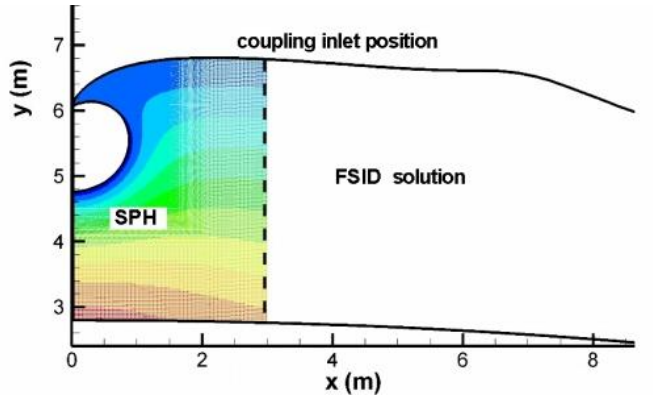

Fig. 11 *– coupling between FSID (global flow) and SPH-flow (local flow interactions during impacts)*

The simulation presented here is based on the coupling with FSID developed by Y.-M. Scolan (Scolan et al., 2007). The flow data are initialized in the SPH domain just before the impact by FSID data. Afterwards, at each time step of the SPH calculation, the flow data in the liquid at the upstream boundary are imposed by FSID. There is no data available in FSID for the gas. So a special boundary condition is set-up for the gas.

For the time being we have not succeeded to get clean simulations of the crest approaching the wall. High velocities (up to 70 m/s) are generated in the air at the free surface close to the tip of the crest and a vortex appears. The depression inside the vortex causes the apparition of void cavities that spoil the flow. Figure 12 shows such a cavity close to the tip of the crest.

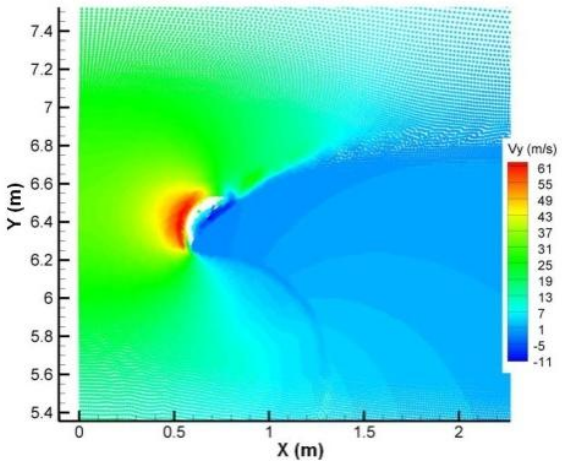

Fig. 12 *– Simulation by SPH-flow of a wave crest approaching a wall while breaking. Apparition of void cavities.*

In order to check the behaviour of the SPH bi-fluid model when the gas pocket is entrapped, a simulation was carried out starting at 8 ms before the crest hits the wall. Doing so, the development of the cavities is avoided as the gas has not enough time to take momentum. Obviously such a modelisation cannot be used for a relevant impact pressure evaluation at the crest level. In these conditions, it gives exactly the same result as the mono-phase simulation performed by Oger et al. (2009).

The model used is composed of 400,000 particles with a minimum distance of 5 mm between particles at the initial time. This is considered as very rough for a determination of a crest impact but sufficient for the simulation of the gas pocket compression.

The compression of the gas pocket is shown in Figure 13 by snapshots colorized by the pressure (left side) and by the velocity modulus (right side) at t=7.5 ms and at t=62.5 ms after the initial instant. Mind that the scales in the liquid phase and the gas phases are not the same.

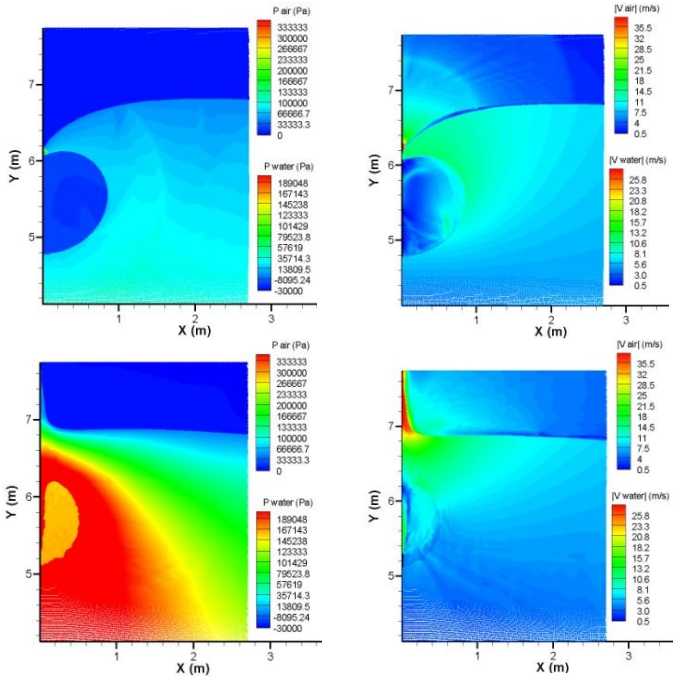

Fig. 13*- Simulation by SPH flow of the compression of a gas pocket entrapped by an impacting wave. Instants t = 0.0075 s, t = 0.0625 s. Left: pressure, right: velocity modulus.*

Figure 14 shows the evolution of the pressure within the gas pocket during the first oscillation.

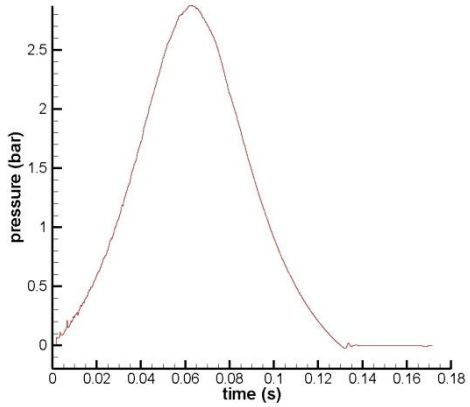

Fig. 14 *– pressure oscillations within a gas pocket entrapped by a wave impact as simulated by SPH-flow.*

When the phase of gas expansion starts at time t=0.13s, the pressure becomes negative in the gas pocket. Then the SPH numerical instability develops, generating a void cavity that prevents a relevant simulation.

CONCLUSIONS

An SPH bi-fluid version of the SPH-flow software is being developed by HydrOcean and ECN, with support from GTT for the special use of liquid impact simulations. An important step forward was achieved recently upgrading the former important capabilities of fluid-structure interaction simulations to the situation where a liquid, a gas and a structure interact together. The parallelization efficiency of the software is conserved at its high initial level.

The code was validated successfully in a situation where the gas is entrapped and cannot escape. The test case considered was the 1D compression of a gas pocket proposed for the Comparative Benchmark Study of ISOPE 2010. The SPH results match exactly with the theoretical results developed by F. Dias (Dias, 2008).

The 2D problem proposed also within the Numerical benchmark simulated by Braeunig et al. in 2009 was simulated. The free fall of an initially rectangular patch of liquid, surrounded by a gas, within a rectangular tank is considered for several configurations. Different fluids and different scales are studied. Similar physical trends are observed qualitatively as those observed during sloshing model tests. For instance, the impact pressures decrease and the impact durations decrease when heavy ullage gas is considered. In situations where the gas cannot escape quickly enough during the approach of the liquid, oscillations of the gas pocket pressure are generated by the model. Furthermore when the simulations are performed at small scale with the scaling situations described by Braeunig et al. as '*Partial Froude Scaling* and *Complete Froude Scaling'* the results match perfectly with Braeunig's conclusions: the impact pressures Froude-scale only when the gas properties are adequately scaled. Otherwise a compressibility bias develops.

The compression of a gas pocket entrapped by a breaking wave onto a wall was also calculated. The first oscillation of the pocket is simulated in a very credible way according to experimental results obtained in different flume tanks.

Nevertheless improvements of the model are needed in order to prevent the development of void cavities when the gas expands or at the centre of vortices and be able to simulate adequately the whole impact phase, including the crest impact.

When such improvements are achieved, some validations with experimental results are scheduled in the case of wave impacts. Such comparisons make sense only when experiments are made in a way that

they provide a good level repeatability of the measured impact pressures. Progress has also been made in this direction recently (Kimmoun et al., 2010), (Bogaert et al., 2010).

GTT's final objective is to compare deterministically single impacts on a rigid structure and on the different membrane containment systems, in order to address the hydro-elasticity issue and to compare single impacts at different scales for Froude-similar in-flow conditions in order to address the scaling issue. We are getting very close to this objective.

ACKNOWLEDGEMENTS

HydrOcean, *GTT* and *ECN* acknowledge:

- the support provided by Y.-M. Scolan (Ecole Centrale de Marseille) making possible the development of the interface between FSID and SPH-flow,
- the computing resources offered by CCIPL, IFREMER and CRIHAN,
- the continuous support of DGA (French Ministry of Defence) in the developments of the SPH-flow fluid solver through *ECN* research contracts

Their help was very much appreciated.

REFERENCES

Bagnold, R., (1939). *Interim report on wave-pressure research*, J. Inst Civil Eng. **12**: 201–226.

Bonet, J., Kulasegaram, S., (2001). "*Remarks on tension instability of Eulerian and Lagrangian corrected smooth particle hydrodynamics (CSPH) methods*", International Journal for Numerical Methods in Engineering , 52, 1203-1220.

Bogaert, H., Brosset, L., Léonard, S., Kaminski, M., (2010). *"Sloshing and scaling: results from Sloshel project"*, 20th (2010) Int. Offshore and Polar Eng. Conf., Beijing, China, ISOPE.

Braeunig, J.-P., Brosset, L., Dias, F., Ghidaglia, J.-M., (2009). "*Phenomenological study of liquid impacts through 2D compressible two-fluid numerical simulations"*, 19th (2009) Int. Offshore and Polar Eng. Conf., Osaka, Japan, ISOPE.

Braeunig, J.-P., Brosset, L., Dias, F., Ghidaglia, J.-M., (2010). "*On the effect of phase transition on impact pressures due to sloshing"*, 20th (2010) Int. Offshore and Polar Eng. Conf., Beijing, China, ISOPE.

Brosset, L., Mravak, Z., Kaminski, M., Collins, S., Finnigan, T., (2009) *"Overview of Sloshel project"*, 19th (2009) Int. Offshore and Polar Eng. Conf., Osaka, Japan, ISOPE.

Colagrossi, A., Landrini, M., (2003). "*Numerical simulation of interfacial flows by Smoothed Particle Hydrodynamics*", Journal of Computational Physics, 191, 448-475

Cueille, P.-V., (2005). "*Modélisation par SPH des phénomènes de diffusion présents dans un écoulement fluide*", PhD Thesis, INSA Toulouse, France.

Deuff, J.-B., (2007). *"Extrapolation au réel des mesures de pressions obtenues sur des cuves modèle réduit"*, PhD Thesis, Ecole Centrale de Nantes/*GTT*, France.

Dias, F., (2008). *"Analytical models for wave impact",* Report for Gaztransport & Technigas, March 2008.

Dias, F., Brosset, L. (2009). *"ISOPE 2010 : Numerical Comparative Study",* on ISOPE web site, Dec. 2009.

Doring, M., (2005). *"Développement d'une méthode SPH pour les applications à surface libre en hydrodynamique"*, PhD Thesis, Ecole Centrale de Nantes, France.

Gray, J., Monaghan, J., Swift, R., (2001). "*SPH elastic dynamics*", Comput. Methods Appl. Mech. Engrg., 190, 6641-6662.

Grenier, N., (2009). *"Modélisation numérique par la méthode SPH de la séparation eau-huile dans les séparateurs gravitaires"*, PhD Thesis, Ecole Centrale de Nantes, France.

Guilcher, P.-M., (2008). *"Contribution au développement d'une méthode SPH pour la simulation numérique des interactions houle-structure"*, PhD Thesis, Ecole Centrale de Nantes, France.

Hu, X. Y., Adams, N. A. *"A multi-phase SPH method for macroscopic and mesoscopic flows"*. J. Comput. Phys. 213 (2006) 844-861.

Kimmoun, O., Ratouis, A., Brosset, L., (2010). *"Sloshing and scaling: experimental study in a wave canal at two different scales"*, 20th (2010) Int. Offshore and Polar Eng. Conf., Beijing, China, ISOPE.

Leduc, J., Marongiu, J.-C., Leboeuf, F., Parkinson, E., (2009) *"Multiphase SPH: A new model based on Acoustic Riemann solver"*, Proc. Of the 4th Spheric Workshop (2009), Nantes, France.

Maillard, S., Brosset, L., (2009) "*Influence of density ratio between liquid and gas on sloshing model tests results*",19th (2009) Int. Offshore and Polar Eng. Conf., Osaka, Japan, ISOPE.

Monaghan, J.J., (1992). *"Smoothed particle hydrodynamics"*, Annu. Rev Astron. Astrophys., 30, 543-574.

Oger, G., (2006). *"Aspects théoriques de la méthode SPH et applications à l'hydrodynamique à surface libre"*, PhD Thesis, Ecole Centrale de Nantes, France.

Oger, G., Doring, M., Alessandrini, B., Ferrant, P., (2006). "*Two-dimensional SPH simulations of wedge water entries*", Journal of Computational Physics, 213, 803-822

Oger, G., Brosset, L., Guilcher, P.-M., Jacquin, E., Deuff, J. –B., Le Touzé, D., (2009) *"Simulations of hydro-elastic impacts using a parallel SPH model"*, 19th (2009) Int. Offshore and Polar Eng. Conf., Osaka, Japan, ISOPE.

Rabczuk, T., Belytschko, T., & Xiao, S. (2004). "*Stable Particle Methods based on Lagrangian Kernels*", Comput. Methods. Appl. Mech. Engrg. , 193, 1035-1063.

Scolan, Y.-M., Kimmoun, O., Branger, H., Remy, F., (2007). *"Nonlinear free surface motions close to a vertical wall. Influence of a local varying bathymetry",* 22nd (2007) Int. Workshop on Water Waves and Floating Bodies, Plitvice, Croatia, IWWWFB.

Swegle, J. W., Hicks D. L., Attaway S. W., (1995). "*Smoothed particle hydrodynamics stability analysis*", Comput. Methods. Appl. Mech. Eng., 116, 123-134.

Van Leer, B., "*Towards the Ultimate Conservative Difference Scheme. V. A Second-Order Sequel to Godunov's Method*". Journal of Computational Physics. 32: 101-136 (1979).

Vila, J.P., (2005) *"SPH Renormalized Hybrid Methods for Conservation Laws: Applications to Free Surface Flows",* Meshfree Methods for Partial Differential Equations II, 43 (2005).

Vila, J.P., (1999) *"On Particle Weighted Methods and Smooth Particle Hydrodynamics",* Mathematical Models and Methods in Applied Sciences (1999).